XMR guided cardiac electrophysiology study and radio frequency ablation

Kawal S. Rhode[*a], Maxime Sermesant[a], Sanjeet Hegde[a], Gerardo Sanchez-Ortiz[b], Daniel Rueckert[b], Reza Razavi[a], Derek L. G. Hill[a]
[a]Division of Imaging Sciences, King's College London, UK.
[b]Department of Computer Sciences, Imperial College London, UK.

ABSTRACT

Introduction: XMR systems are a new type of interventional facility in which patients can be rapidly transferred between x-ray and MR systems on a floating table. We have previously developed a technique to register MR and x-ray images obtained from such systems. We are carrying out a programme of XMR guided cardiac electrophysiology study (EPS) and radio frequency ablation (RFA).
Aim: The aim of our work was to apply our registration technology to XMR guided EPS/RFA in order to integrate anatomical, electrophysiological and motion information. This would assist in guidance and allow us to validate and refine electromechanical models.
Method: Registration of the imaging modalities was achieved by a combination of system calibration and real-time optical tracking. Patients were initially imaged using MR imaging. An SSFP volume scan of the heart was acquired for anatomical information, followed by tagged scans for motion information. The patients were then transferred to the x-ray system. Tracked biplane x-ray images were acquired while electrical measurements were made from catheters placed in the heart. The relationship between the MR and x-ray images was determined. The MR volume scan of the heart was segmented and the tagged scans were analysed using a non-rigid registration algorithm to compute motion. The position of catheters was reconstructed within the MR cardiac anatomy. The anatomical, electrophysiological, and motion information were displayed in the same coordinate system. Simulations of electrical depolarisation and contraction were performed using electromechanical models of the myocardium.
Results: We present results for 2 initial cases. For patient 1, a contact mapping system was used for the EPS and for patient 2, a non-contact mapping system was used.
Conclusions: Our XMR registration technique allows the integration of anatomical, electrophysiological, and motion information for patients undergoing EPS/RFA. This integrated approach has assisted in interventional guidance and has been used to validate electromechanical models of the myocardium.

Keywords: Cardiovascular intervention, optical tracking, 2D-3D registration, XMR systems, electrophysiology study, radio frequency ablation, electromechanical models

1. INTRODUCTION

1.1 Clinical background

Cardiac arrhythmias are the cause of considerable morbidity and even occasional mortality. Tachyarrhythmias (fast heart rhythms) can originate from ectopic foci of electrical depolarisation or from abnormal conduction pathways in the myocardium. Also, patients that have suffered a myocardial infarction can have regions of scarring that lead to areas of slowed conduction or total conduction block. These regions can lead to asynchrony of ventricular contraction. This can contribute to the heart failure seen following myocardial infarction.

The treatment of choice for patients with tachyarrhythmias is radio-frequency ablation (RFA) [1]. During RFA procedures, the abnormal electrical focus or pathway is ablated by applying radio-frequency energy to the endocardial surface through the tip of a special catheter that has been inserted into the appropriate chamber of the heart. For patients with ventricular asynchrony, the treatment of choice is biventricular pacing. In this procedure pacing wires are inserted into the heart via a delivery catheter and then connected to a pacing device.

[*] ksr@compuserve.com; phone +44 (0) 207 955-5000 ext 5725; fax +44 (0) 207 955 4532; www-ipg.umds.ac.uk

In order to determine the site of RFA or pacing wire placement, an electrophysiology study (EPS) is performed. During an EPS, a specially designed electrical measurement catheter is inserted into the appropriate chamber of the heart and the electrical activity on the endocardial surface is measured. For RFA procedures the site of the abnormal focus or pathway can be determined from this electrical map, and for biventricular pacing procedures, the optimal location of the pacing wires can be determined as can the optimal pacing strategy.

1.2 Cardiac electrical mapping systems

There are several commercial systems available for carrying out EPS. They can be divided into two categories, firstly contact mapping systems, and secondly non-contact mapping system. Contact mapping systems employ direct contact between measurement electrodes and the endocardium, whereas non-contacting mapping systems do not have direct contact but utilise extrapolation algorithms to extend electrical measurements made within the cardiac chambers to the endocardial surface.

The contact mapping system supplied by Boston Scientific[1] employs the Constellation catheter, a multi-electrode basket catheter (Fig. 1). The basket consists of 8 splines along each of which 8 electrodes are placed, making a total of 64 electrodes. The splines are flexible and the basket is initially folded into the catheter bore and expands when deployed from the tip of the catheter. The splines adapt to the endocardial surface and deform so that contact is maintained as the cardiac chamber contracts through the cardiac cycle. Electrical measurements can then be made for the region of myocardium in contact with the electrodes and the electrograms are displayed as a series of graphical traces. Applications of this type of mapping system can be found in [2-3].

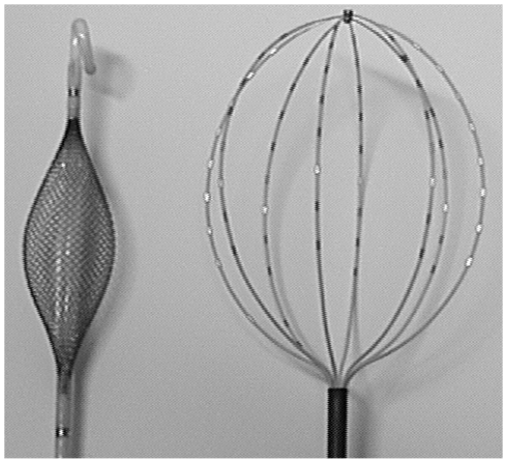

Fig. 1. (left) Endocardial Solutions Inc. balloon catheter. (right) Constellation catheter.

Fig. 2. XMR suite at Guy's hospital.

Endocardial Solutions, Inc. (E.S.I.) [2] supplies the EnSite non-contact electrical mapping system. This employs a catheter containing a flexible balloon made from a wire mesh (Fig. 1). The balloon is initially folded into the catheter bore and expands on deployment. It floats inside the desired cardiac chamber and does not contact the endocardial surface. The wire mesh intersection points on the balloon serve as electrodes and measure the electrical activity within the chamber. A second catheter, known as the roving catheter, is also inserted into the chamber. This catheter emits a radio-frequency signal from its tip that is detected by multiple sensors on the balloon. The location of the tip relative to the balloon is calculated using triangulation. The roving catheter is used to map the endocardial surface of the chamber by moving the catheter over this surface. The electrical activity measured by the balloon is then extrapolated to this surface and displayed by colour coding a surface rendering. The location of the roving catheter tip can be seen relative to the reconstructed endocardial surface and this catheter can be used to deliver radio-frequency energy for ablation or used to deliver pacing signals. Applications of this type of mapping system can be found in [4-5].

[1] www.bostonscientific.com
[2] www.endocardial.com

Biosense Webster[3] supplies a contact mapping system known as CARTO. This is similar to the EnSite system in that it creates a surface representation of the target cardiac chamber. This is done be using a weak electromagnetic field to locate a roving catheter with respect to another reference catheter. The roving catheter can be moved along the endocardial surface whilst acquiring the electrical and the positional information simultaneously. The electrical information is then colour coded on a surface rendering. Applications of this type of mapping system can be found in [6-7].

1.3 Procedure guidance

EPS, RFA procedures, and insertion of pacing wires are carried out under x-ray fluoroscopic guidance. This type of guidance has several advantages for these procedures. The catheters employed are designed to be x-ray visible and can be seen throughout the part of their length that lies in the field of view since x-ray imaging is a projection imaging modality. Also, since images can be acquired rapidly (typically 25 frames per second), cardiac motion does not cause significant motion artifacts. However, there are some disadvantages that have a significant impact on the catheter guidance and image interpretation. Firstly, since x-ray imaging is a projection imaging modality, more than one view is necessary to gain an appreciation of the three-dimensional location and path of catheters. Therefore, these procedures are often carried out using biplane x-ray systems. Secondly, the anatomical context of the acquired images can be difficult to interpret since soft tissues, such as the heart and the great vessels, are not visible during x-ray exposure. Therefore, the positioning of catheters for electrical measurement, RFA, or pacing can be difficult using x-ray guidance. Furthermore, the interpretation of the electrical signals from the electrical mapping catheters, such as the Constellation catheter, and of the relationship of these signals to the anatomical context from x-ray images alone requires considerable expertise. Although generation of reconstructed endocardial surfaces by the EnSite and the CARTO systems has made a step forward in assisting with this problem, the accuracy with which these surfaces can be generated is complicated by problems such as cardiac and catheter motion. EPS and RFA procedures are often lengthy in duration due to the difficulties outlined, and this can lead to prolonged x-ray dose to the patient and the staff carrying out these procedures.

We are currently undertaking a programme of XMR guided EPS and RFA procedures. XMR systems are a recently introduced interventional imaging solution in which an x-ray system and a MR system are placed in the same interventional room (or adjoining rooms with large sliding doors between). Patients can be rapidly transferred between the two imaging modalities on a common floating table. Although this is the commonest configuration, another configuration has been reported in which the x-ray system is integrated into the MR system [8]. XMR systems are designed to provide a migration path to MR guided intervention. MR imaging has several advantages over x-ray imaging for guidance. Firstly, MR imaging provides high quality anatomical information and excellent three-dimensional visualisation of cardiovascular structures. Secondly, it is also possible to obtain functional information such as chamber volumes, blood flow, and cardiac wall motion. Finally, there is no ionising radiation delivered to the patient. However, devices that are used during interventions, such as catheters, are not designed to be MR visible or compatible as they often contain ferromagnetic materials or long electrical conductors. Much effort is being directed into making devices MR compatible and visible although the routine use of such devices in patients is still to be established. Many procedures have been successfully carried out using MR guidance in animal models [9-10] and our group has reported the first clinical use of MR catheter guidance [11]. However, the migration of EPS and RFA procedures to MR guidance is still a long way in the future.

1.4 Aims

For our current clinical programme, we aimed to use hybrid MR and x-ray imaging for guidance of EPS and RFA procedures. The strategy of our approach is to perform the procedure using x-ray guidance with pre- and post-procedure MR imaging to determine patient cardiac anatomy and wall motion. Using an XMR registration technique that we have previously developed [12-13], we aimed to combine the MR images with the x-ray images to provide an integrated representation of the patient that can be used for interventional guidance. Furthermore, we aimed to simulate myocardial electrical depolarisation and contraction using electromechanical models of the myocardium and our integrated representation of the patient anatomical, electrical, and motion data. In this paper we present results from two clinical cases. In the first case we show how our technique can be applied to an EPS carried out with a Constellation catheter, and for the second case, to an EPS carried out with the EnSite system.

[3] www.biosensewebster.com

2. METHOD

2.1 Description of XMR facility

The XMR interventional suite (Fig. 2) at King's College London (Guy's Hospital Campus) comprises an x-ray and RF shielded room, with positive pressure air handling for sterility. The room contains a 1.5 T cylindrical bore MR scanner (Philips Intera I/T) and a mobile cardiac x-ray set (Philips BV Pulsera). The patient can be easily moved between the two systems using a specially modified sliding MR table top that docks with and transfers patients to a specially modified x-ray table (Philips Angio Diagnost 5 Syncratilt table). The docking and transfer takes less than 60 seconds. We have previously described the use of this system for guiding interventions on patients with congenital heart disease [11].

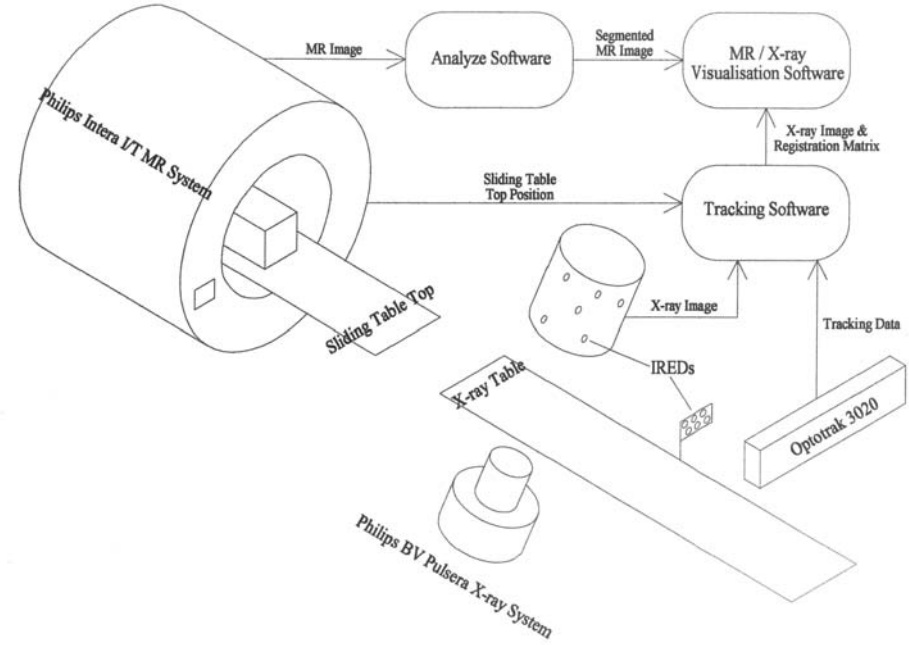

Fig. 3. Components of the tracking and registration system.

2.2 XMR registration technique

Although it is possible to acquire MR images and x-ray images of the same patient during a procedure, the XMR system has no inherent ability to register these images. We have previously described the validation of a novel XMR registration technique [12-13] that is applicable to the sliding table XMR configuration. A registration technique has also been described for fixed table configuration [14]. Our technique is based on tracking the moving components of the XMR system, i.e. the sliding table top, the x-ray table, and the x-ray c-arm. The position of the sliding table top is automatically displayed by a linear position readout while it is docked to the MR system. The x-ray table and the x-ray c-arm are tracked using optical tracking. Six infrared emitting diodes are fixed to these components and the location of these is monitored by a Northern Digital Optotrak 3020. In order to register MR and x-ray images acquired during an intervention, the system must be initially calibrated. Calibration is performed using an acrylic calibration object that accepts specially developed interchangeable markers that are visible in both MR and x-ray images and that can be located using a pointing device and the Optotrak. The calibration object is fixed to the sliding table and imaged using both modalities and the marker positions are found using the Optotrak pointing device. Using this information the geometric relationship between the MR and x-ray systems can be determined as can the projection geometry of the x-ray system. Once a calibration has been performed, it is possible to acquire MR and tracked x-ray images during interventions and to compute the registration matrix that maps the points in 3D MR image space to 2D x-ray image space. Using the registration matrix it is then possible to display a rendering of the patient's cardiac anatomy derived from the MR images overlaid on the acquired x-ray images. Furthermore, using biplane x-ray images and the epipolar constraint [15] it is possible to reconstruct the location of devices seen in the x-ray images, such as measurement

electrodes and catheters, in the MR derived patient cardiac anatomy. An overview of the tracking and registration system is shown in Fig. 3.

2.3 Patient details and image acquisition

2.3.1 Clinical case 1

Patient 1, male aged 15, had an intermittent ventricular tachycardia that was to be treated by EPS and RFA. The patient underwent paralysis and general anaesthesia prior to the procedure. Initially, MR imaging was performed. The cardiac anatomy was acquired using an SSFP three-dimensional multiphase sequence (5 phases, 256x256 matrix, 152 slices, resolution=1.33 mm x 1.33 mm x 1.4 mm, TR=3.0 ms, TE=1.4 ms, flip angle=45°). Myocardial motion imaging was performed in both short axis (SA) and long axis (LA) views using a SPAMM tagged imaging sequence (59 phase SA & 50 phases LA, 256x256 matrix, 11 slices SA & 4 slices LA, resolution=1.33 mm x 1.33 mm x 8.0 mm, TR=11.0 ms, TE=3.5 ms, flip angle=13°, tag spacing=8 mm). The patient was then transferred to the x-ray system. Four electrical measurement catheters were inserted into the patient's right ventricle. Three of these were multipolar catheters and the fourth was a Constellation basket catheter. Dynamic biplane tracked x-ray images were acquired with the catheters in place and at the same time the electrical activity was recorded from the Constellation catheter during two ventricular ectopic beats. The x-ray image acquisition was carried out using ventilator control at end expiration to match the phase of ventilation during which the MR images were acquired. The patient then underwent a successful RFA.

2.3.2 Clinical case 2

Patient 2, male, aged 68, had poor left ventricular function following a myocardial infarction. The patient was to undergo EPS and programmed pacing to assess the optimal location of pacing wires for biventricular pacing. The patient underwent sedation and local anaesthesia. Initially, MR imaging was performed. The cardiac anatomy was acquired using an SSFP three-dimensional multiphase sequence (3 phases, 256x256 matrix, 120 slices, resolution=1.48x1.48x1.0mm, TR=3.2ms, TE=1.6ms, flip angle=45°). Myocardial motion imaging was performed in both short axis and long axis views using a CSPAMM spiral tagged imaging sequence (35 phases, 256x256 matrix, 9 slices SA & 5 slices LA, resolution=1.76x1.76x12.0mm, TR=13.0ms, TE=1.1ms, flip angle=30°, tag spacing=6mm). The patient was then transferred to the x-ray system. Three electrical measurement catheters were inserted into the patient's heart. One was a quadrapole catheter that was placed in the right ventricle; one was the EnSite system's balloon catheter that was placed in the left ventricle; and the other was a decapole catheter that acted as the EnSite system's roving catheter that was also placed in the left ventricle. Initially, the roving catheter was moved along the endocardial surface of the left ventricle and the EnSite system tracked its position to generate a surface representation of this chamber. The electrical activity was then measured by the balloon catheter and visualised on the reconstructed left ventricular surface. Dynamic biplane tracked x-ray images were acquired with the catheters in place. Furthermore, the locations of the 4 most distal electrodes on the roving catheter with reference to the EnSite coordinate system were recorded. The x-ray imaging was carried out using end expiration breath holding to match the phase of respiration in which the MR images were acquired. The patient then underwent programmed pacing and had a successful pace maker implantation at a later date.

2.4 Catheter reconstruction and visualisation

For each of the two patients, the MR SSFP 3D heart images were transferred from the MR scanner to a workstation. They were segmented to isolate the anatomy of interest using the Analyze software package (Mayo Clinic, Minnesota, USA). For patient 1, the right heart was segmented, and for patient 2, the left heart was segmented. Although several phases were available through the cardiac cycle, the end diastolic phase was selected for visualisation. Phase matching of the acquired x-ray images to the MR images was performed manually by selecting the end diastolic x-ray images. The segmented MR anatomy was overlaid onto the x-ray images using the registration matrices for each x-ray view. Furthermore, the 3D locations of the catheters that were visible in the x-ray images were reconstructed using biplane x-ray views, the registration matrices and the epipolar constraint. This was carried out semi-automatically [16]. The reconstructed catheter paths were displayed in the segmented MR cardiac anatomy. For patient 1, the location of each of the 64 electrodes in the Constellation catheter was found with reference to the segmented MR anatomy. Although this was performed by manually clicking each of the electrodes in the biplane views, an automated technique has been proposed [17].

2.5 Mapping the electrical data to the patient anatomy

For patient 1, electrical recordings were made from the electrodes of the Constellation catheter. The recordings were bipolar so that the 64 electrodes produced 32 electrograms with measurement taking place between successive electrodes along each spline. The electrograms were extracted from the measurement system. The position of the 64 electrodes of the Constellation catheter in the MR image space has already been determined. We triangulated this point cloud by using the position of neighbouring electrodes to obtain a surface representing the area covered by the basket catheter. Surface to image registration was carried out to correct any error in the alignment of the basket surface and the segmented MR anatomy. Such misalignment may arise due to patient motion and errors in the registration process. The surface to image registration was performed using an Iterative Closest Point algorithm, as proposed by [18]. For each vertex of the basket mesh, we computed the corresponding boundary voxel in the MR image. The MR image is segmented so the boundary voxels could be defined based on the gradient value. For each vertex of the basket surface, the corresponding point in the MR image was found by looking for a boundary point along the normal to the basket surface. The comparison of the gradient direction at this voxel with the vertex normal gives another criterion to confirm if the voxel found is the correct boundary point. Then from all the matched vertex/boundary point pairs we estimated the best rigid body transformation between the Constellation catheter surface and the MR image and this process was iterated until convergence. Once the registration has been refined, the signals from the electrograms were displayed by colour coding the basket surface.

For patient 2, the EnSite system produced a surface representation of the left ventricle. This was available for further processing as 256 sampled points with corresponding electrograms. Initially, we registered the EnSite system surface to the segmented MR anatomy. A landmark based registration technique has been reported [19] but we rely on our XMR registration technology. We needed to perform a rigid body registration to align the coordinate system of the EnSite surface and the MR volume. Since the location of the distal 4 electrodes of the roving catheter were measured in the EnSite coordinate system and also determined in the MR coordinate system, it was possible to compute this rigid body transform. Furthermore, the origin of the EnSite coordinate system lies at the centre of the balloon catheter. It was possible to compute the location of this point in the MR coordinate system using the registered biplane x-ray views, making a total of 5 points that were used to find the transformation relating the two coordinate systems. Since the surface given by the EnSite system is an estimation of the end-diastolic endocardium, its shape will not exactly match the left ventricular MR anatomy. Also, there will be errors in the alignment of the EnSite surface and the MR anatomy due to patient motion and errors in the registration process. Therefore, we deformed the ESI surface to better match the MR image to allow us to proceed with our analysis. This was performed using the deformable surfaces framework [20], where the surface to be deformed evolves under the influence of two energies: an external energy aiming to adjust the surface to the image and an internal energy that keeps the surface regular. For each vertex of the surface, the corresponding point in the image is found by looking for a boundary point along the normal of the surface as described earlier. Then a force is applied on the surface proportional to the distance between the vertex and the corresponding boundary point. The dynamics equation is solved using an internal energy smoothing the surface by minimising the area locally, thus the curvature, as proposed in [21]. Since the location of the poles of the balloon catheter are known with some confidence from the catheter reconstruction process, the corresponding poles of the EnSite surface were constrained to be fixed during the deformation. It was then possible to display the electrograms on both the original and deformed EnSite surfaces.

2.6 Extraction of myocardial motion

The myocardial motion was extracted by analysis of the tagged MR images. A non-rigid registration approach was used in the analysis [22-23]. Since the motion information is in the MR coordinate system, we now have registered anatomical, electrical, and motion data.

2.7 Simulation of electrical depolarisation and myocardial contraction

Since electrical data was measured for the whole of the left ventricle in patient 2, it was possible to use the registered anatomical, electrical, and motion data for investigating electromechanical models of the myocardium. Simulation of the cardiac electro-physiology is usually done using either the Luo-Rudy [24] type of model or the FitzHugh-Nagumo [25] type. The former is based on the simulation of all the different ions present in a cardiac cell along with the different ion channels. The latter is based on a more global scale, only modeling the potential difference between the intracellular and the extracellular space (the action potential). As we are interested in the timing of the depolarisation propagation and

intend to interpret it in terms of local conductivity, we used a FitzHugh-Nagumo type of model. Moreover, Luo-Rudy variables are not observable *in vivo* and much too numerous to be adjusted from our data. We used the adapted version for cardiac cells of the FitzHugh-Nagumo equations proposed by [26]. We solved these equations on a volumetric tetrahedral mesh to compute a whole myocardium propagation and on a triangulated surface to simulate the propagation on the endocardium. We also introduced the muscle fibre directions in the computation, as they intervene in the propagation speed. More details about the electrical model can be found in [27]. The simulated depolarisation was compared to the measured depolarisation using isochrones.

The action potential controls the mechanical contraction of the myocardium. To simulate this phenomenon, the constitutive law for the myocardium must include an active element, responding to an action potential by developing a contraction stress. We used the model presented in [28] and based on multi-scale modeling of the myocardium detailed in [29]. This model is a combination of a transverse anisotropic, piecewise linear visco-elastic passive constitutive law with an active element creating a contraction stress tensor. Once the cardiac motion was simulated, we compared the displacement of the vertices of the model with the displacement extracted from the tagged MR images.

3. RESULTS

3.1 Clinical case 1

Fig. 4 shows the biplane x-ray images used to reconstruct the catheter and basket electrode positions and two corresponding views of the segmented MR anatomy containing the reconstructed structures. Fig. 5 shows the surface mesh generated from the basket electrode points and same mesh transformed rigidly to match the segmented MR anatomy. Fig. 6 shows motion vectors computed from the tagged MR images and the registered basket catheter. Fig. 7 shows the progression of depolarisation during a ventricular ectopic beat.

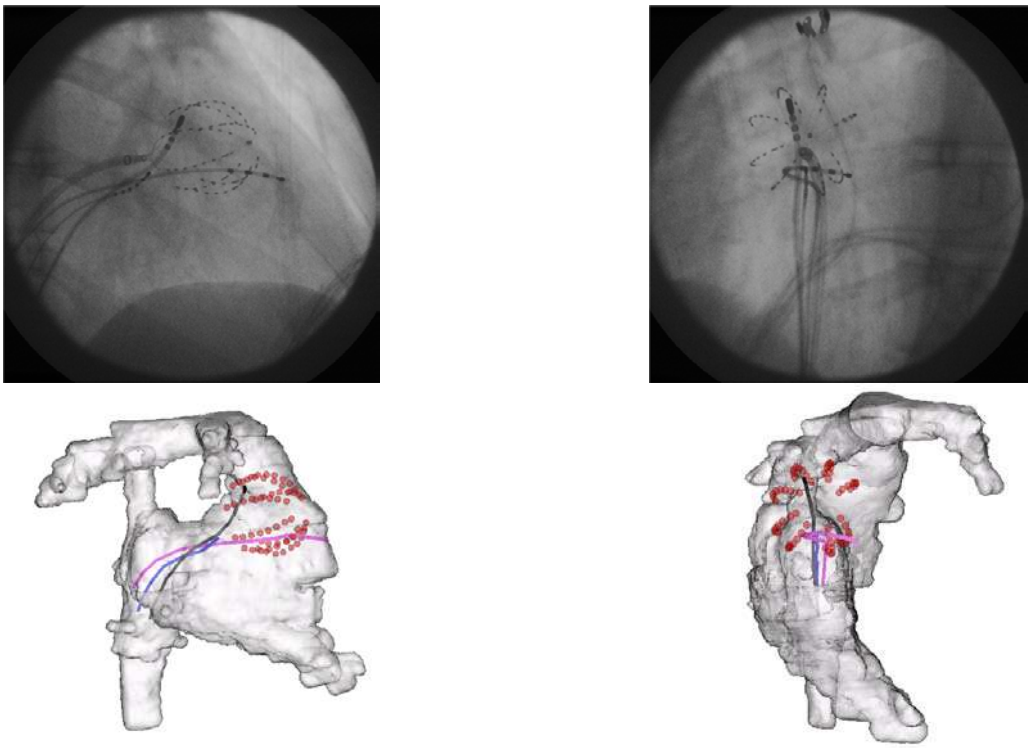

Fig. 4. Patient 1: Four catheters are visible in the biplane x-ray views placed in the right ventricle. Three are multipole linear catheters and the fourth is a Constellation catheter. The path of the catheters and the electrode positions are displayed in the segmented MR anatomy of the right heart.

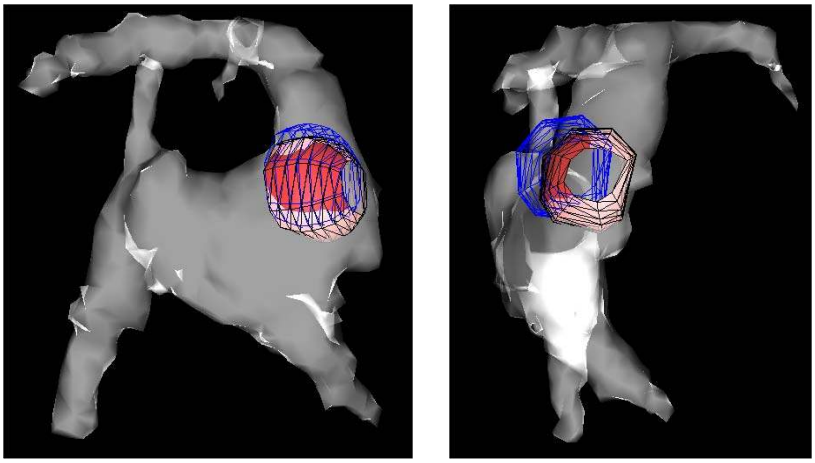

Fig. 5. Patient 1: The positioned of the mesh generated from the Constellation catheter electrode points is shown before and after rigid body deformation.

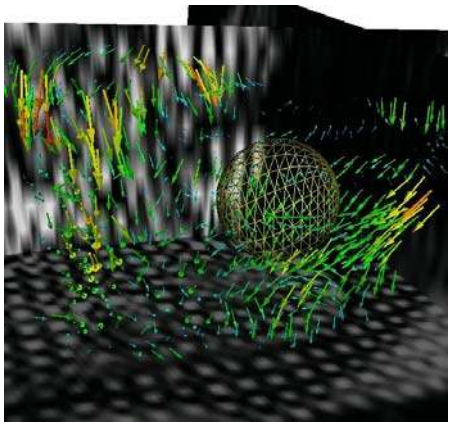

Fig. 6. Patient 1: Tagged image slices & computed motion vectors in the right ventricle for one cardiac phase, and the Constellation basket in the same coordinate system.

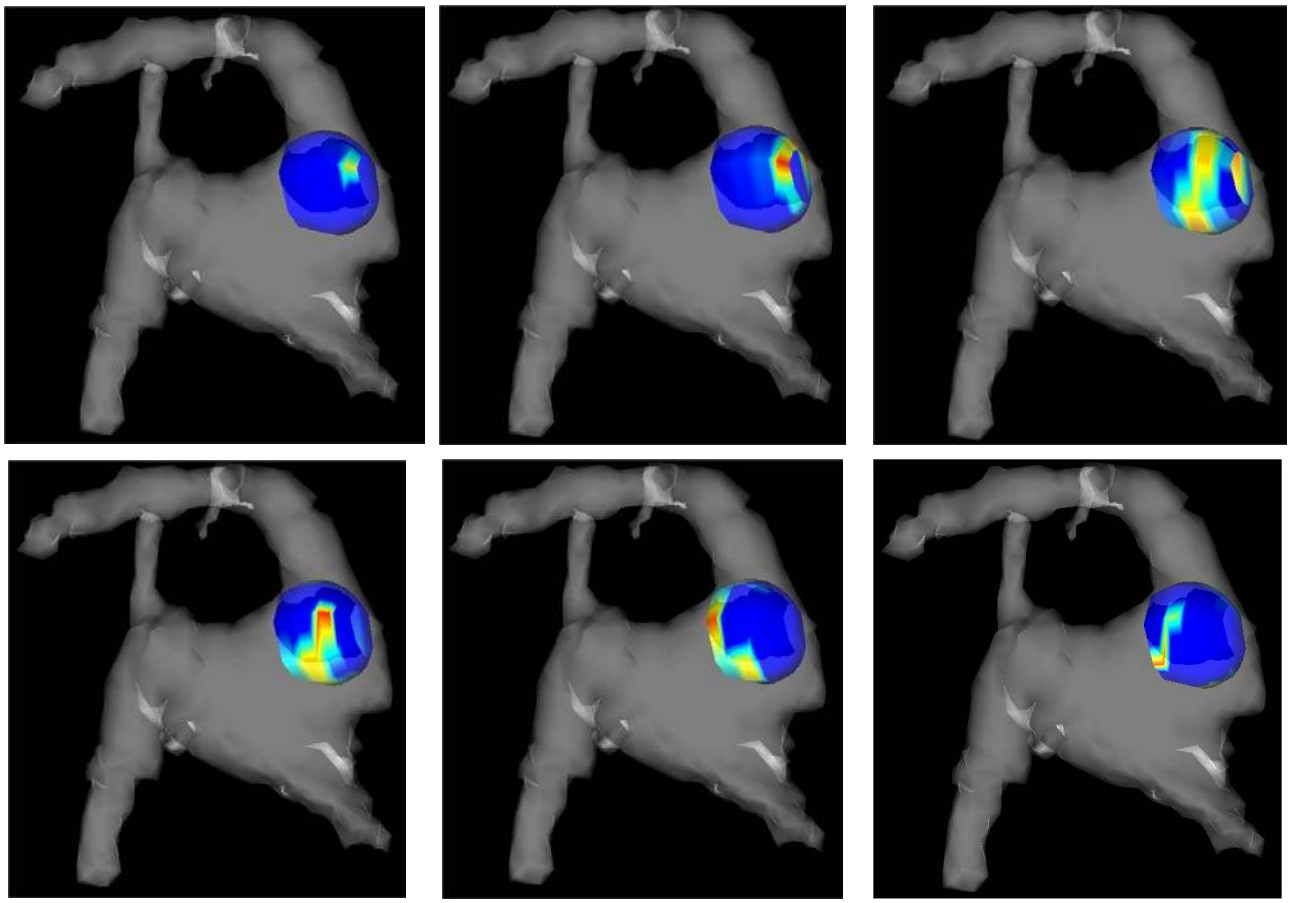

Fig. 7. Patient 1: The progression of depolarisation during an ectopic beat arising from the right ventricular outflow tract. The ectopic focus can be seen in the first frame.

3.2 Clinical case 2

Fig. 8 shows the biplane x-ray images used to reconstruct the catheter positions and two corresponding views of the segmented MR anatomy containing the reconstructed catheters. Fig. 9 shows the original EnSite system surface registered to the segmented MR anatomy and the deformed EnSite surface. Fig. 10 shows the measured and the simulated electrical depolarisation mapped onto the deformed EnSite surface. Fig. 11 shows the isochrones computed from the measured electrograms and those computed from the simulated depolarisation. Also the difference in the isochrones is illustrated. Fig. 12 illustrated the myocardial motion computed from the tagged MR images and that computed from the simulation.

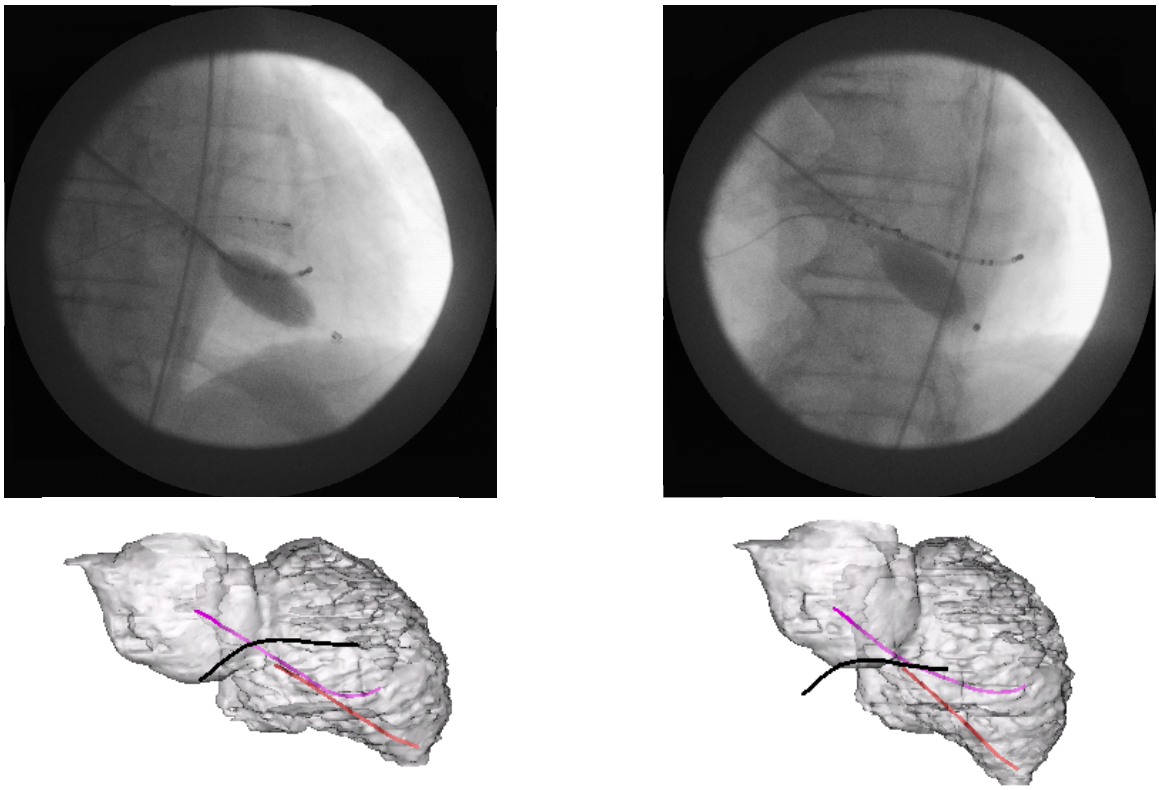

Fig. 8. Patient 2: Three catheters are visible in the biplane x-ray views. The quadrapole catheter was placed in the right ventricle, and the decapole and balloon catheters were placed in the left ventricle. The path of these catheters is shown in the segmented MR anatomy.

Fig. 9. Patient 2: (left) The EnSite surface is shown registered to the segmented MR anatomy. (right) The deformed EnSite surface is shown along with the initial registered surface.

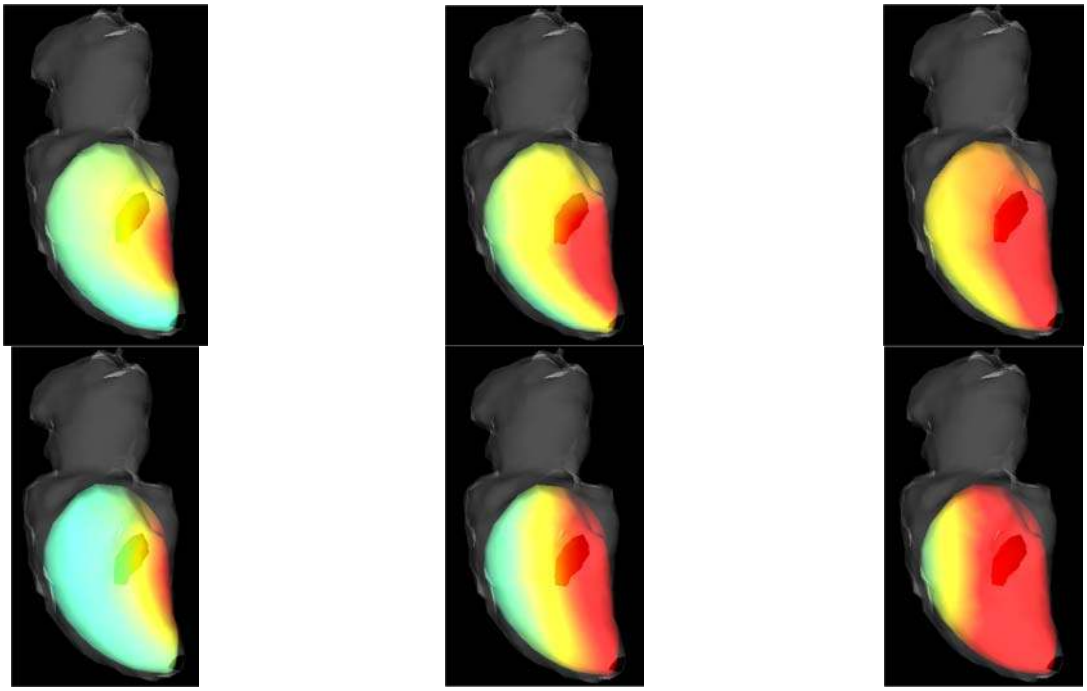

Fig. 10. Patient 2: The measured (top) and the simulated (bottom) electrical depolarisation for three phases of the cardiac cycle.

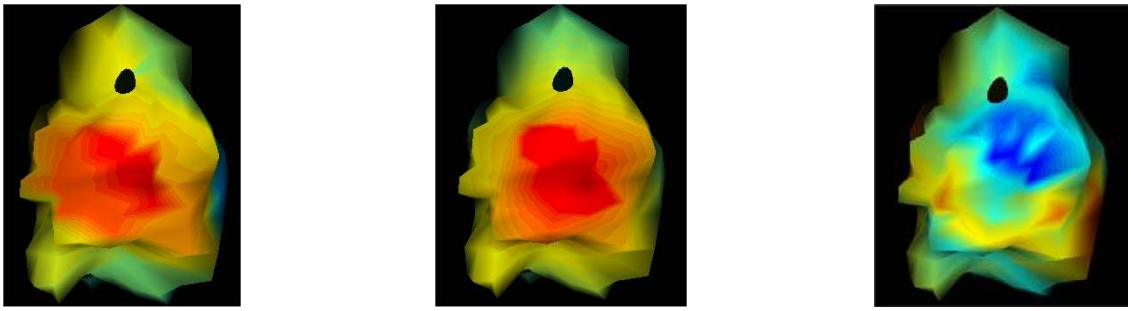

Fig. 11. Patient 2: Isochrones computed from the measured (left) and simulated (centre) electrical data shown on the original EnSite surface and the difference image (right).

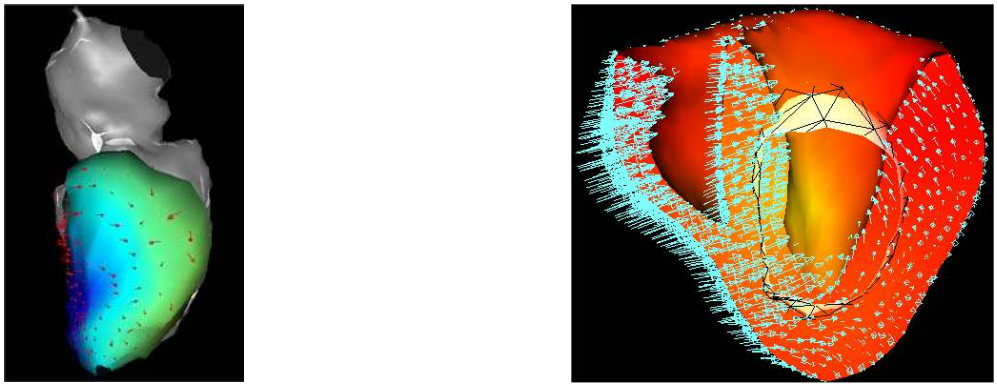

Fig. 12. Patient 2: (left) The simultaneous display of anatomical and measured electrical and motion data. (right) The display of simulated electrical and motion data in the modeling reference volumetric mesh.

4. DISCUSSION & CONCLUSIONS

We have proposed a method to integrate anatomical, electrophysiological, and myocardial motion data for patients undergoing electrophysiology study in the XMR environment using our XMR registration technology. We have demonstrated how this integrated representation can be further used to validate electromechanical models of the myocardium. Our integrated representation has several potential benefits. Firstly, overlaying MR derived anatomical surface renderings of the heart and great vessels onto x-ray images acquired during procedures will aid in interventional guidance allowing easier positioning of catheters. Secondly, the ability to reconstruct catheter locations in the MR anatomy will allow verification of catheter position, which could potentially be of benefit for the accurate location of ablation and pacing catheters. Thirdly, the ability to map measured electrical data onto patient specific anatomy would facilitate the diagnosis of electrical conduction abnormalities. This would have a significant impact on investigations carried out using basket catheters, such as the Constellation catheter, where no anatomical context is available and the procedure outcome relies heavily on the expertise of the cardiologists and electrophysiology technicians. As well as providing additional information for the staff carrying out EPS and RFA procedures, these benefits could reduce procedure time and thus radiation dose, which is particularly important for paediatric cases. We have presented our initial results in two clinical cases. For the case using the EnSite system, we were able to carry out some initial simulation studies. The ability to model the electrical depolarisation and the contraction of the myocardium could be used to simulate the outcome of RFA or different pacing strategies. Furthermore, the availability of registered electrical and motion data in patients will allow us to validate the electromechanical models and potentially refine these models using the measured data. In on going work we are improving the accuracy of our registration technology and developing a quantitative approach to the comparison of measured and simulated electromechanical data. In the longer term, it is possible that the combination of anatomical and motion information from MRI with a validated electromechanical model will enable the site requiring ablation or pacing to be identified non-invasively.

ACKNOWLEDGMENTS

The authors acknowledge the UK-EPSRC (Grant JR/R41019/1), the UK Medical Imaging and Signals IRC, the UK JREI, Philips Medical Systems and the Charitable Foundation of Guy's & St Thomas' Hospitals for funding. The authors acknowledge the contributions of Dr. E. Rosenthal, Dr. C. Bucknall, Dr. P. Lambiase, D. Elliott, and E.S.I. Also, the authors acknowledge the use of the MIPS software from the Epidaure project, INRIA, France.

REFERENCES

1. J. Hebe, P. Hansen, F. Ouyang, M. Volkmer, K. H. Kuck, "Radiofrequency catheter ablation of tachycardia in patients with congenital heart disease," *Pediatr. Cardiol.*, 21(6), pp. 557-75, 2000.
2. M. Eldar, D. G.Ohad, J. J. Goldberger, Z. Rotstein, S. Hsu, D. K. Swanson, A. J. Greenspon, "Transcutaneous multielectrode basket catheter for endocardial mapping and ablation of ventricular tachycardia in the pig," *Circulation*, 96(7), pp. 2430-7, 1997.
3. C. Schmitt, B. Zrenner, M. Schneider, M. Karch, G. Ndrepepa, I. Deisenhofer, S. Weyerbrock, J. Schreieck, A. Schomig, "Clinical experience with a novel multielectrode basket catheter in right atrial tachycardias," *Circulation*, 99(18), pp. 2414-22, 1999.
4. K. Okishige, M. Kawabata, S. Umayahara, K. Yamashiro, M. Gotoh, M. Isobe, S. A. Strickberger, "Radiofrequency catheter ablation of various kinds of arrhythmias guided by virtual electrograms using a noncontact, computerized mapping system," *Circ. J.*, 67(5), pp. 455-60, 2003.
5. P. D. Lambiase, A. Rinaldi, J. Hauck, M. Mobb, D. Elliott, S. Mohammad, J. S. Gill, C. A. Bucknall, "Non-contact left ventricular endocardial mapping in cardiac resynchronisation therapy," *Heart*, 90(1), pp. 44-51, 2004.
6. L. Gepstein, G. Hayam, S. A. Ben-Haim, "A novel method for nonfluoroscopic catheter-based electroanatomical mapping of the heart. In vitro and in vivo accuracy results," *Circulation*, 95(6), pp. 1611-22, 1997.
7. J. L. R. M. Smeets, S. A. Ben-Haim, L-M. Rodriguez, C. Timmermans, H. J. J. Wellens, "New method for nonfluoroscopic endocardial mapping in humans. Accuracy assessment and first clinical results," *Circulation* 97(24), pp. 2426-2432, 1998.
8. R. Fahrig, K. Butts, J. A. Rowlands, R. Saunders, J. Stanton, G. M. Stevens, B. L. Daniel, Z. Wen, D. L. Ergun, N. J. Pelc, "A truly hybrid interventional MR/x-ray system: feasibility demonstration," *J. Magn. Reson. Imaging,* 13(2), pp. 294-300, 2001.

9. A. Buecker, J. M. Neuerburg, G. B. Adam, A. Glowinski, T. Schaeffter, V. Rasche, J. J. van Vaals, A. Molgaard-Nielsen, R. W. Guenther, "Real-time MR fluoroscopy for MR-guided iliac artery stent placement," *J. Magn. Reson. Imaging,* 12(4), pp. 616-22, 2000.
10. A. Buecker, E. Spuentrup, R. Grabitz, F. Freudenthal, E. G. Muehler, T. Schaeffter, J. J. van Vaals, R. W. Gunther, "Magnetic resonance-guided placement of atrial septal closure device in animal model of patent foramen ovale," *Circulation,* 106 (4), pp. 511-515, 2002.
11. R. Razavi, D. L. Hill, S. F. Keevil, M. E. Miquel, V. Muthurangu, S. Hegde, K. Rhode, M. Barnett, J. van Vaals, D. J. Hawkes, E. Baker, "Cardiac catheterisation guided by MRI in children and adults with congenital heart disease," *Lancet*, 362(9399), pp. 1877-82, 2003.
12. K. S. Rhode, D. L. Hill, P. J. Edwards, J. Hipwell, D. Rueckert, G. Sanchez-Ortiz, S. Hegde, V. Rahunathan, R. Razavi, "Registration and tracking to integrate X-ray and MR images in an XMR facility," *IEEE Trans. Med. Imaging*, 22(11), pp. 1369-78, 2003.
13. K. S. Rhode, D. L. G. Hill, P. J. Edwards, J. Hipwell, D. Rueckert, G. Sanchez-Ortiz, S. Hegde, V. Rahunathan, R. Razavi, "Application of XMR 2D-3D registration to cardiac interventional guidance," in *Proc. MICCAI*, vol. 2878, pp. 295-302, 2003.
14. H. Yu, R. Fahrig, N. J. Pelc, "Co-registration of X-ray and MR fields of view in a truly hybrid system," in *Proc. Intl. Soc. Mag. Reson. Med.*, 11, 2003.
15. D. J. Hawkes, A. C. F. Colchester, C. Mol, "The accurate 3D reconstruction of the geometric configuration of vascular trees from x-ray recordings*,"* in *Physics and Engineering of Medical Imaging*, Ed. Guzzardi, Martinus Nijhoff, The Hague, 1985.
16. K. S. Rhode, T. Lambrou, D. J. Hawkes, G. Hamilton, A. M. Seifalian, "Validation of an optical flow algorithm to measure blood flow waveforms in arteries using dynamic digital x-ray images," in *Proc. SPIE, Medical Imaging*, vol. 3979, pp. 1414–1425, 2000.
17. I. H. de Boer, F. B. Sachse, and O. Doessel, "A model based approach for localization of basket catheters for endocardial mapping," in *Proc. CARS*, pp 1004, 2000.
18. J. Montagnat, H. Delingette, "Globally constrained deformable models for 3D object reconstruction," *Signal Processing*, 71(2): pp. 173–186, 1998.
19. Z. J. Malchano, R. C. Chan, G. Holmvang, E. J. Schmidt, A. d'Avila, T. J. Brady, J. N. Ruskin, V. Y. Reddy, "Registration strategies for alignment of cardiac MR data with 3D electrophysiology maps," in *Proc. Intl. Soc. Mag. Reson. Med.*, 11, 2003.
20. J. Montagnat, H. Delingette, "A review of deformable surfaces: topology, geometry and deformation," *Image and Vision Computing*, 19(14), pp. 1023–1040, 2001.
21. M. Desbrun, M. Meyer, P. Schröder, A. Barr, "Implicit fairing of arbitrary meshes using diffusion and curvature flow," in *International Conference on Computer Graphics and Interactive Techniques (ACM Siggraph'99)*, pp. 317–324, ACM Press/Addison-Wesley, 1999.
22. R. Chandrashekara, R. H. Mohiaddin, D. Rueckert, "Analysis of myocardial motion in tagged MR images using non-rigid image registration," in *Proc. SPIE, Medical Imaging,* vol. 4684, pp. 1168-1179, 2002.
23. G. Sanchez-Ortiz, R. Chandrashekara, K. S. Rhode, R. Razavi, D. L. G. Hill, D. Rueckert, "Detecting regional changes in myocardial contraction patterns using MRI," in *Proc. SPIE, Medical Imaging*, 2004.
24. C. Luo, Y. Rudy, "A model of the ventricular cardiac action potential: depolarization, repolarization, and their interaction," *Circ. Res.*, 68, pp. 1501–1526, 1991.
25. R. FitzHugh, "Impulses and physiological states in theoretical models of nerve membrane," *Biophysical Journal*, 1, pp. 445–466, 1961.
26. R. Aliev, A. Panfilov, "A simple two-variable model of cardiac excitation," *Chaos, Solitons & Fractals*, 7(3), pp. 293–301, 1996.
27. M. Sermesant, O. Faris, F. Evans, E. McVeigh, Y. Coudière, H. Delingette, N. Ayache, "Preliminary validation using *in vivo* measures of a macroscopic electrical model of the heart," in *International Symposium on Surgery Simulation and Soft Tissue Modeling (IS4TM'03)*, 2003.
28. M. Sermesant, Y. Coudière, H. Delingette, N. Ayache, "Progress towards an electro-mechanical model of the heart for cardiac image analysis," in *IEEE International Symposium on Biomedical Imaging (ISBI'02)*, 2002.
29. J. Bestel, F. Clément, M. Sorine, "A biomechanical model of muscle contraction," in *Proc. MICCAI*, vol. 2208, pp. 1159–1161, Springer, 2001.